Proceedings of the XII International Symposium on Dynamic Problems of Mechanics (DINAME 2007),
Varoto, P. S. and Trindade, M. A. (Editors), ABCM, Ilhabela, SP, Brazil, February 26 - March 2, 2007

Diagnosis of cracked shafts by monitoring the transient motion response

Christian Rodríguez Burbano[1], Valder Steffen, Jr[2]

[1] Occidental de Colombia Inc. Calle 77A No. 11-32 Bogotá – Colombia. 57-1-6069339 . ext: 3389

[2] School of Mechanical Engineering, Federal Univ. of Uberlândia, Campus Santa Mônica, 3400-902 Uberlândia - Brazil

Abstract: This study addresses the problem predicting faults in flexible rotors by using changes due to the presence of cracks in the vibration behavior of the system in the transient motion. The response of a rotor consisting of a shaft containing a rigid disc located in the mid point of the shaft was obtained. A crack in the same rotor was experimentally introduced by using an electro-erosion process. The severity (depth / shaft diameter) of the crack was 0.5. The transient motion response was measured by using eddy probes installed in the proximity of the disc surface. The experimental vibration behavior of the rotor was analyzed for two different situations, with and without crack. The natural frequencies of the system were obtained by impact testing along two vibration directions (horizontal and vertical). The finite element method was used to model the rotor. For the cracked shaft, the stiffness matrix corresponding to the cracked element was obtained by using the Mayes model. The stiffness coefficients of the bearings were identified by an inverse problem technique using Genetic Algorithms. The transient motion response was numerically integrated by using the Newmark's method. The numerical response was then compared with the experimental one for validation purposes. Simulations for different balancing conditions, crack severity and acceleration rate were performed. As a conclusion, it was found that a cracked shaft exhibits important changes on the orbit when the rotor is passing through rotation speeds equal to ¼, ⅓, and ½ the critical speed. Besides, the analysis of the vibration response in time domain is sometimes more useful than the orbit analysis to identify changes related to cracks in rotors.

Keywords: cracked shaft, transient motion, flexible rotors

NOMENCLATURE

a = crack depth
aa = crack severity a/d
c = damping
c_{ij} = flexibility coefficient in i caused by a force in j.
$[C]$ = damping matrix
$[C_c]$ = flexibility matrix cracked element
$[C_1]$ = Additional flexibility matrix
D = disc diameter
d = shaft diameter
l = length of the cracked element
$f(t)$ = step function
F1= unbalance force
F2= unbalance force
$[G]$ = gyroscopic matrix
J = energy density function
K_I, K_{II}, K_{III} = stress intensity factors
$K_{\eta\eta}$ = stiffness in η
$[K]$ = stiffness matrix
m = mass
$[M]$ = mass matrix
U = strength energy

Greek Symbols

β = unbalance mass angle
Δh = additional flexibility
α = crack surface section
η = rotating coordinates axis.
ε = eccentricity
ϕ = position angle
ξ = rotating coordinate axis

Subscripts

c relative to cracked shaft
e relative to element
0 relative to pristine condition

INTRODUCTION

The diagnostic of rotating machinery using vibration monitoring is based on the idea that any change on the machinery behavior is caused by an operation condition change or a mechanical condition change. There are some excitations that are always present in rotating machinery, such as unbalance and misalignment. These excitation forces together with dynamic efforts associated to the machine operation will result fatigue. Material defects blended with fatigue stresses may end in a rotor failure (this can happen in long or short time). Then, it is clear that rotor failure is always a possibility in rotating machinery. This possibility cannot be completely eliminated, however we can monitor the rotors looking for small faults before they cause major damage.

A crack is a failure with higher potential damage. Because of that, the search for new methods to find and detect early stage cracks has been active during the last thirty years (Penny and Friswell, 2003). Direct methods, such as ultra-sonic, magnetic particles, and penetrant liquid, are very popular, however they exhibit a significant disadvantage: they

require stopping the machine. This is an important drawback because industrial plants are supposed to be efficient and frequent stops are very costly. In this context some researchers have been studying the vibration behavior of cracked shafts for diagnostics purposes. As a result, various crack models have been developed and it was found some unique vibration behavior for cracked shafts, namely the sub-harmonic resonance (Nelson and Nataraj, 1986). One of the most important phenomena regarding cracked shafts is the so-called "breathing". It occurs in cracked shafts for the cases in which unbalance forces are lower than rotor weight, therefore the crack opens and closes agreeing with both magnitude and direction forces acting on the crack section (Dimarogonas and Paipetis, 1983).

In this paper a theoretical and experimental behavior of a cracked rotor is described. The experimental rotor test rig used is a steel shaft with a rigid disc located in the shaft mid point, supported in the ends by bearings. This rotor is F.E.M. modeled and genetic algorithms are used to identify the bearing parameters. The stiffness matrix for the cracked element is derived from the Mayes crack model. Theoretical results are compared with experimental ones for the transient motion of the system. It is found that changes in the shaft orbits when passing through 1/3, ½ of the critical speed and changes in the values of structural resonance can be used as indicators for cracked shafts diagnostic (Darpe and Grupta, 2003).

Theory

Crack models Description

To explain the crack model a Laval rotor is described, according to the following equations of motion:

$$\begin{bmatrix} m & 0 \\ 0 & m \end{bmatrix}\begin{Bmatrix} \ddot{\eta} \\ \ddot{\xi} \end{Bmatrix} + \dot{\phi}\begin{bmatrix} 0 & -2m \\ 2m & 0 \end{bmatrix}\begin{Bmatrix} \dot{\eta} \\ \dot{\xi} \end{Bmatrix} + \begin{bmatrix} c & 0 \\ 0 & c \end{bmatrix}\begin{Bmatrix} \dot{\eta} \\ \dot{\xi} \end{Bmatrix} + \underbrace{\begin{bmatrix} K_{\eta\eta} & K_{\eta\xi} \\ K_{\xi\eta} & K_{\xi\xi} \end{bmatrix}}_{K}\begin{Bmatrix} \eta \\ \xi \end{Bmatrix} + \begin{bmatrix} 0 & -c\dot{\phi} \\ c\dot{\phi} & 0 \end{bmatrix}\begin{Bmatrix} \eta \\ \xi \end{Bmatrix} +$$

$$+\begin{bmatrix} -\dot{\phi}^2 m & 0 \\ 0 & -\dot{\phi}^2 m \end{bmatrix}\begin{Bmatrix} \eta \\ \xi \end{Bmatrix} = \begin{Bmatrix} m.\varepsilon.\dot{\phi}^2\cos(\beta) - mg\cos(\phi) + \ddot{\phi}m\varepsilon\, sen(\beta) \\ m.\varepsilon.\dot{\phi}^2 sen(\beta) + mg\, sen(\phi) - \ddot{\phi}m\varepsilon\cos(\beta) \end{Bmatrix} \quad (1)$$

The crack geometry is shown in the figure (1).

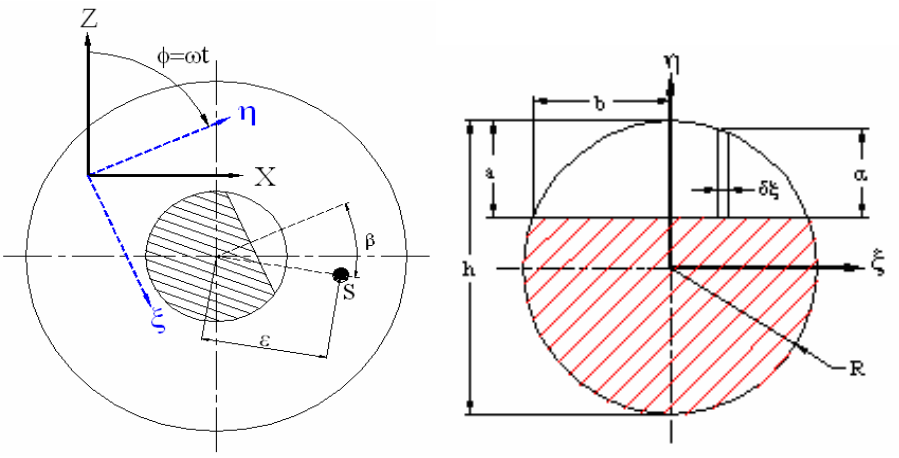

Figure 1 – Coordinate systems and Crack geometry.

Matrix [K] in the equation (1) is the stiffness matrix. The main effect of a crack in a shaft is the stiffness variation. The way stiffness varies characterizes the differences found in the models of cracked shafts. The present contribution considers that the most significant models of cracked shafts are the following:

Gash model (hinge Model): This model was developed regarding low severity cracks. In this kind of cracks, the influence of flexibility in the cross axis, ξ, is negligible, therefore it is not considered. This model only considers the additional flexibility in the main crack axis, η (Gash,R. 1993). For this model there are only two crack states, open and closed. The crack state depends on a function value, which is a function of η. In rotating coordinates this model is expressed as in the following (Darpe, A.K. and Gupta, K. 2003):

$$\begin{Bmatrix}\eta\\ \xi\end{Bmatrix} = \left(\underbrace{\begin{bmatrix} h_0 & 0 \\ 0 & h_0 \end{bmatrix}}_{\substack{uncracked\ shaft \\ flexibility}} + f(t) \underbrace{\begin{bmatrix} \Delta h_{\eta,\max} & 0 \\ 0 & 0 \end{bmatrix}}_{\substack{additional\ flexibility \\ with\ open\ crack}} \right) \begin{Bmatrix} f_\eta \\ f_\xi \end{Bmatrix} \tag{2}$$

where:

$$f(t) = \begin{cases} 0 \\ 1 \end{cases} \begin{matrix} for & \eta \le 0 \\ for & \eta > 0 \end{matrix} \tag{3}$$

When f(t)=0, no additional flexibility is taken into account, and the stiffness matrix is the same for the non-cracked shaft. The flexibility matrix depends on the rotor response and the equations of motion become nonlinear. Figure 2 shows the stiffness variation along a shaft revolution.

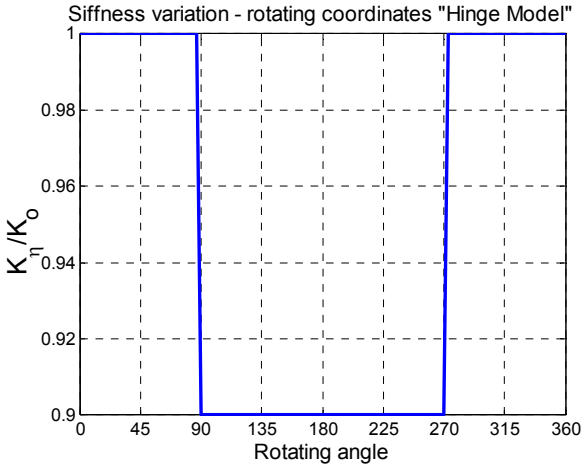

Figure 2 – Stiffness variation in a shaft revolution (Gash model)

Mayes Model: In this model the stiffness variation in rotating coordinates is defined by the following expressions:

$$K_\eta(\phi) = \frac{1}{2}(K_0 + K_\eta) + \frac{1}{2}(K_0 - K_\eta)\cos(\phi) \tag{4}$$

and

$$K_\xi(\phi) = \frac{1}{2}(K_0 + K_\xi) + \frac{1}{2}(K_0 - K_\xi)\cos(\phi) \tag{5}$$

Therefore, the stiffness matrix in rotating coordinates is:

$$K_R = \begin{bmatrix} K_\eta(\phi) & 0 \\ 0 & K_\xi(\phi) \end{bmatrix} \tag{6}$$

The stiffness matrix with respect to inertial coordinates is given by:

$$K_F = \begin{bmatrix} c_1^{\,2}K_\eta + s_1^{\,2}K_\xi & s_1c_1(K_\xi - K_\eta) \\ s_1c_1(K_\xi - K_\eta) & s_1^{\,2}K_\eta + c_1^{\,2}K_\xi \end{bmatrix} \tag{7}$$

where $c_1 = \cos(\phi)$ and $s_1 = sen(\phi)$

Figure 3 shows the stiffness variation in rotating coordinates.

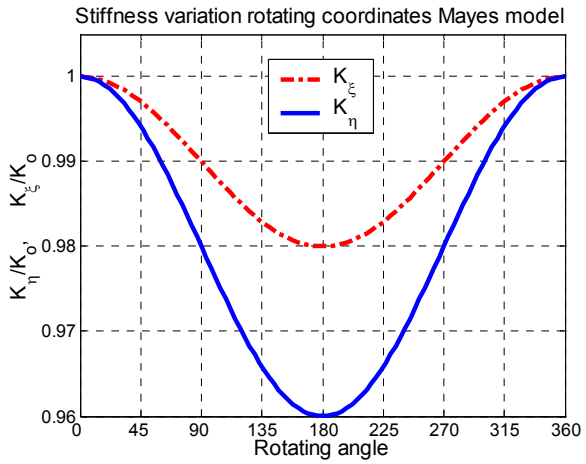

Figure 3 - Stiffness Variation in rotating coordinates (Mayes model)

Switching Model: This model considers only two crack states: totally open or totally closed. It can be considered as a Gash model improvement, for which the stiffness depends on the rotor response along the crack main axis, η. The main difference with respect to the Gash model is that it considers the stiffness variation along the perpendicular directions, η and ξ. The equations of motion for this model for a constant angular velocity, $\dot{\phi} = \Omega$, are given below (Jun et al. 1992b):

$$m(\ddot{\eta} - 2\Omega\dot{\xi} - \Omega^2\eta) + c(\dot{\eta} - \Omega\xi) + \left[K_0 - \frac{K_0 - K_\eta}{2}\{1 + \mathrm{sgn}(\eta)\}\right]\eta = m\varepsilon\Omega^2\cos(\beta) - mg\cos(\Omega t) \tag{8}$$

$$m(\ddot{\xi} + 2\Omega\dot{\eta} - \Omega^2\xi) + c(\dot{\xi} + \Omega\eta) + \left[K_0 - \frac{K_0 - K_\xi}{2}\{1 + \mathrm{sgn}(\eta)\}\right]\xi = m\varepsilon\Omega^2 sen(\beta) + mgsen(\Omega t) \tag{9}$$

The stiffness variation in rotating coordinates is shown in figure 4.

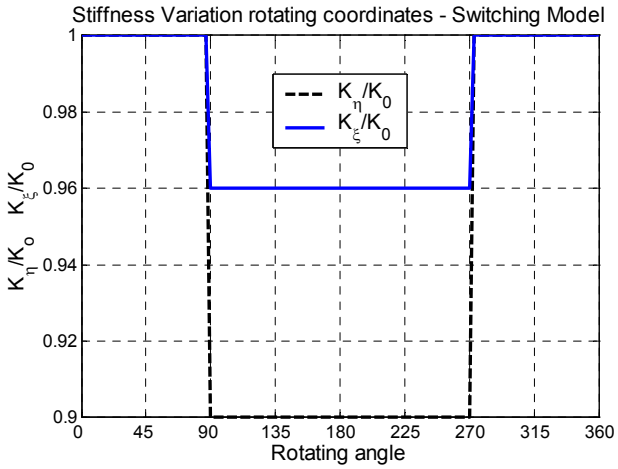

Figure 4 – Stiffness Variation in rotating coordinates (Switching model)

Breathing based on fracture mechanics: This model is intended to represent the cracked model behavior accordingly, but has the disadvantage of requiring significant computational effort. First, the model determines how much the crack is open (in other words, the model is able to consider partially opened cracks). For doing this, it is necessary to calculate the stress intensity factors (Anderson, 1995), which can be obtained for a cracked shaft by using the following expression:

$$K_{ni} = \sigma_i\sqrt{\pi\alpha}F_n\left(\frac{\alpha}{h}\right) \tag{10}$$

where α is the crack depth.

The flexibility coefficients are obtained according to equation (11) and the additional flexibility matrix jis given by equation (12) (Oller, S. 2001).

$$c_{ij} = \frac{\partial^2}{\partial P_i \partial P_j} \int_{-b}^{b} \int_{0}^{\alpha} J(\alpha) d\alpha d\xi \tag{11}$$

$$F_{crack} = \begin{bmatrix} c_{11} & 0 & 0 & c_{14} & c_{15} & 0 \\ 0 & c_{22} & 0 & 0 & 0 & c_{26} \\ 0 & 0 & c_{33} & 0 & 0 & c_{36} \\ c_{41} & 0 & 0 & c_{44} & c_{45} & 0 \\ c_{51} & 0 & 0 & c_{54} & c_{55} & 0 \\ 0 & c_{62} & c_{63} & 0 & 0 & c_{66} \end{bmatrix} \tag{12}$$

Application of Mayes Model using F.E.M

The flexibility coefficients are calculated by using the fracture mechanics theory, considering only flexion forces. Then, both axial displacement and axial forces are negligible. For the case in which the crack is located in center of the element, the total flexibility matrix is obtained through equation (13), and the stiffness element matrix is given by equation (14), (Saavedra, 2002). Finally, as the working reference system adopted in the present work is the inertial one, the stiffness element matrix has to be expressed in this reference.

$$[C_C] = [C^1] + [C^0] \tag{13}$$

$$[K_C]^e = [\Pi][C_C]^{-1}[\Pi]^T \tag{14}$$

Where,

$$[\Pi]^T = \begin{bmatrix} -1 & 0 & 0 & 0 & 0 & 0 & 1 & 0 & 0 & 0 & 0 & 0 \\ 0 & -1 & 0 & l & 0 & 0 & 0 & 1 & 0 & 0 & 0 & 0 \\ 0 & 0 & -1 & 0 & -l & 0 & 0 & 0 & 1 & 0 & 0 & 0 \\ 0 & 0 & 0 & -1 & 0 & 0 & 0 & 0 & 0 & 1 & 0 & 0 \\ 0 & 0 & 0 & 0 & -1 & 0 & 0 & 0 & 0 & 0 & 1 & 0 \\ 0 & 0 & 0 & 0 & 0 & -1 & 0 & 0 & 0 & 0 & 0 & 1 \end{bmatrix} \tag{15}$$

Equation 6 has to be integrated to obtain the transient motion response. Notice that the stiffness matrix depends on the rotating angle and Mayes model is then applied. Regarding the FEM implementation, equation (16) is to be integrated (Lalanne and Ferraris, 1998).

$$[M]\{\ddot{\delta}\} + \left([C] + [G]\dot{\phi}\right)\{\dot{\delta}\} + \left([K_1(\phi)] + [K_2]\ddot{\phi}\right)\{\delta\} = \dot{\phi}^2\{F_1(\phi)\} + \ddot{\phi}\{F_2(\phi)\} \tag{16}$$

The experimental rotor test rig

A 15.875 mm diameter steel shaft is used. The 297.5mm length shaft is supported in the ends by ball bearings. A rigid disc of 140 mm diameter and 15 mm thick was mounted with 0.001" of interference at the shaft mid point. It has sixteen equally spaced ¼" holes, which are used to install balancing weights. In order to read the rotor response (displacement), eddy probes SKF CMSS68 were installed along the vertical and horizontal directions. As the shaft diameter is rather small, the eddy probes were installed to work over the disc lateral surface, thus avoiding cross influence between horizontal and vertical readings. A 2HP AC motor with a speed control board drives the rotor. The speed control is done manually. Experimental data are acquired with an acquisition card and stored in files to be processed into Matlab® for further analysis. The cracked shaft was obtained from the non-cracked one by introducing an 8 mm crack in the shaft. The crack was generated by an electric-erosion process, through which a crack surface gap of 0.3mm was left. The rotor run-out was read over the lateral surface of the disc for both the cracked and non-cracked rotors. As machining errors causes the run-out, it was removed from the final readings during the analysis process.

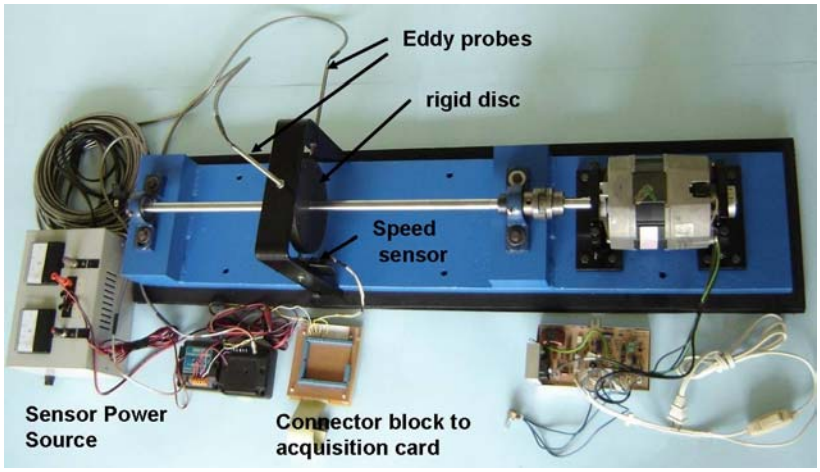

Figure 5 – Rotor Test-Rig

Rotor model

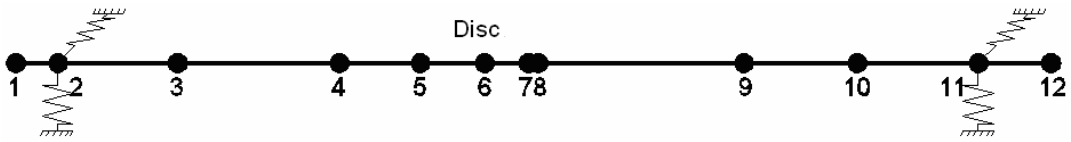

Figure 6 – Rotor discretization by FEM

The rotor was modeled using the finite element method FEM with twelve nodes as shown in Fig. 6. An impact test was performed for the non-cracked rotor, resulting a natural frequency of 44.738 Hz in the horizontal direction and 44.394 Hz in the vertical direction. These values were used to update the rotor model with respect to the bearing stiffness coefficients (K_{xx}, K_{yy}). These values were obtained through an inverse problem by using genetic algorithms. For this purpose, the objective function was expressed by equation (16).

$$F = (44.738 - w_{nx})^2 + (44.3942 - w_{ny})^2 \tag{16}$$

Experimental Results

In order to study the influence of the severity and orientation of the crack, unbalance responses performed for various unbalance conditions. For the transient motion analysis, data for different acceleration rates were considered. Impact tests in the horizontal and vertical directions were performed to study the variation of the natural frequencies due to the crack. The crack was aligned with the impact direction and also perpendicularly to this direction for each impact and the results in the time domain are shown the Fig. 8. It is clear that the first effect of the crack in the shaft is a stiffness reduction, and it is also clear that the lowest stiffness occurs when the crack main axis coincides with the evaluating axis. Looking for changes in the natural frequencies has been used since many years ago for crack diagnostics, however its main inconvenient in rotating machinery is that the bump test requires that the object be stopped, because this it is more used in large structures than in rotating machinery.

The transient motion vibration for the cracked shaft has shown higher amplitude values than the non-cracked shaft. These large amplitudes occur in a lower rotating speed as compared with the non-cracked shaft, due to stiffness reduction. One of the most important characteristics of a cracked shaft as mentioned by a number of authors is the so-called sub-harmonic resonance when the rotating speed is ½, 1/3, ¼ of the critical speed. This behavior was verified in this study and it was found that the acceleration rate has an important influence in the rotor response. The changes in the rotor response when sub-harmonic resonance occurs is less evident for high acceleration rates than for low acceleration rates. Both time domain responses and orbits are good crack indicators in the passing through sub-harmonic resonance, as can be seen in Figure 9. It could be concluded that the difference between a cracked and non-cracked rotor is that the response amplitude is more evident when the rotor is in the ½ critical speed than for other sub-harmonic situations. The orbits obtained for the non-cracked rotor are the typical ones for the case in which unbalance is the only excitation force. The differences between vertical and horizontal direction responses are due to stiffness differences. This means that for

an unbalanced symmetric rotor the expected orbit is a circle and the time response is a sine wave. The time response and the orbit for the non-cracked rotor when passing through ½ critical speed are showed in Fig. 10.

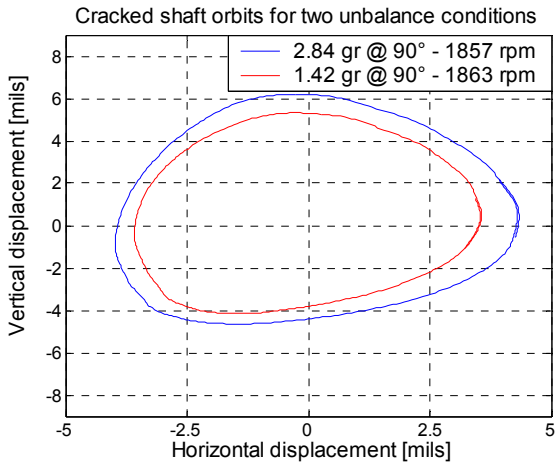

Figure 7 – Cracked rotor orbits for 1.42 gr @ 90°and 2.84 gr@90° unbalance.

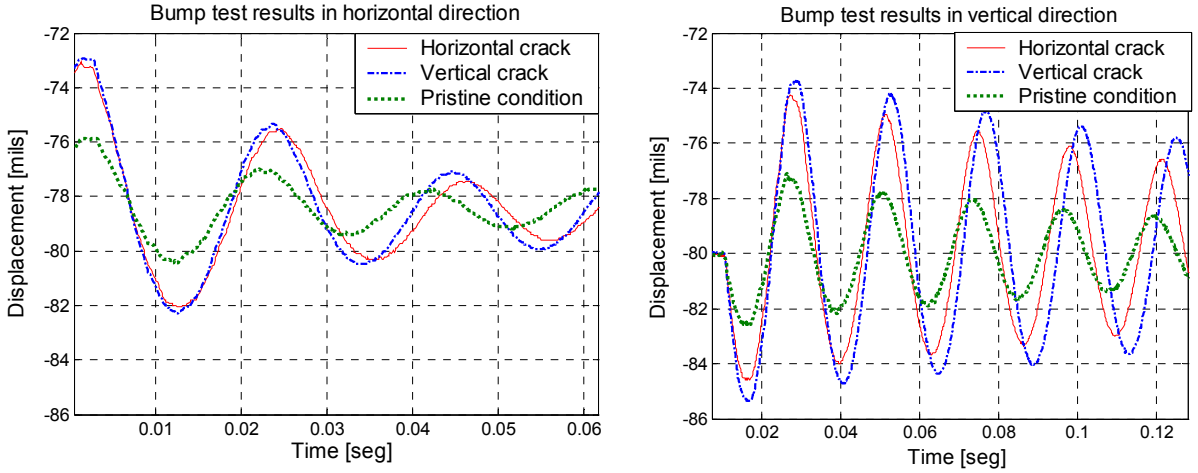

Figure 8 – Impact test results for the pristine condition rotor and cracked rotor in time domain.

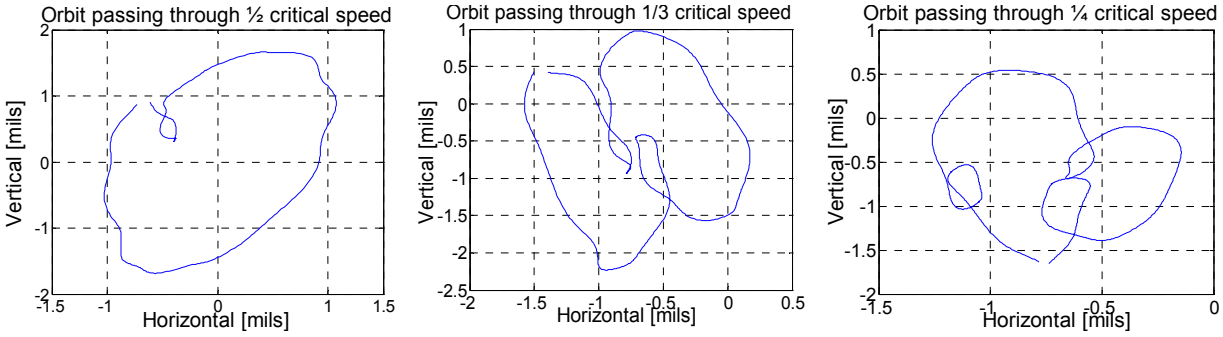

Figure 9 – Cracked rotor orbits passing through ¼,1/3 and ½ critical speed

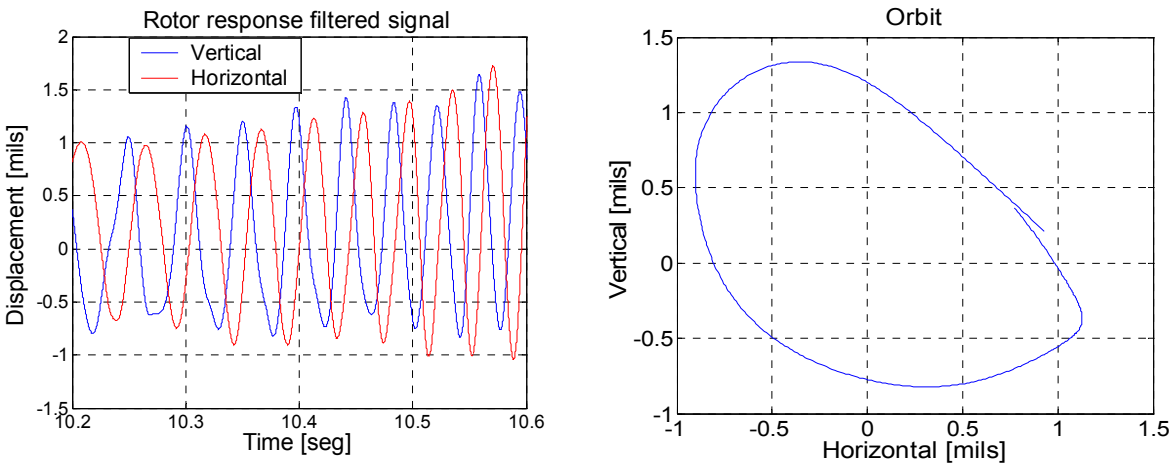

Figure 10 – Pristine condition rotor time response and orbit passing through ½ critical speed.

Theoretical response of both cracked and pristine condition shaft in the transient motion

To integrate Eq. (16), the Runge Kutta method was first used, however the results were not satisfactory. Then, as the Newmark's method was previously used (Bathe and Wilson, 1976) successfully by other researchers for transient motion studies (Pacheco R.P, 1996), it was implemented in the present contribution. The time increment used was 0.00005 seconds, and for the cracked shaft the stiffness matrix had to be calculated for each angular position where the rotor response is evaluated. The procedure used to calculate the non-cracked rotor response is the same without having to calculate the stiffness matrix to each angular position, i.e., the stiffness matrix is constant. A computer code written in Matlab® was developed to calculate the rotor response.

To evaluate the model behavior, the excitation force used in the simulations is same unbalance (same unbalance mass and angle) used in the experimental tests. The main characteristics observed in the experimental results such as higher amplitudes at lower rotating speeds and the sub-harmonic resonances were also observed in the simulations, as shown in Figures 11 and 12. The theoretical amplitudes differ a little from the experimental ones. In the opinion of the authors, this is possibly due to the acceleration rates there were not the same for both cases, however an important reason to be considered is related to the damping coefficients that were not identified and have high influence in the rotor response when passing through the critical speed. However, the model is able to represent the orbits form accordingly, i.e., they match the experimental results. It can be considered that the mathematical model represents adequately the differences observed experimentally between the cracked and the pristine case, being suitable to the study of the dynamic behavior of cracked rotors.

Simulations were performed to evaluate the influence of crack severity crack in the rotor response. It was found that for crack severities lower than 0.2, the difference between a cracked and a non-cracked shaft is imperceptible. In Fig. 13 the results presented demonstrate this point.

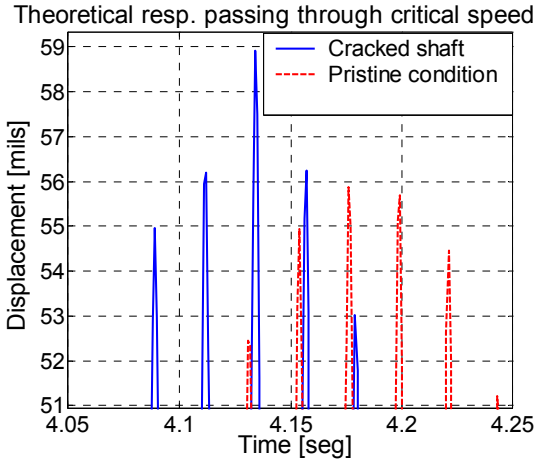

Figure 11 – Theoretical response for cracked and pristine condition rotor passing through critical speed

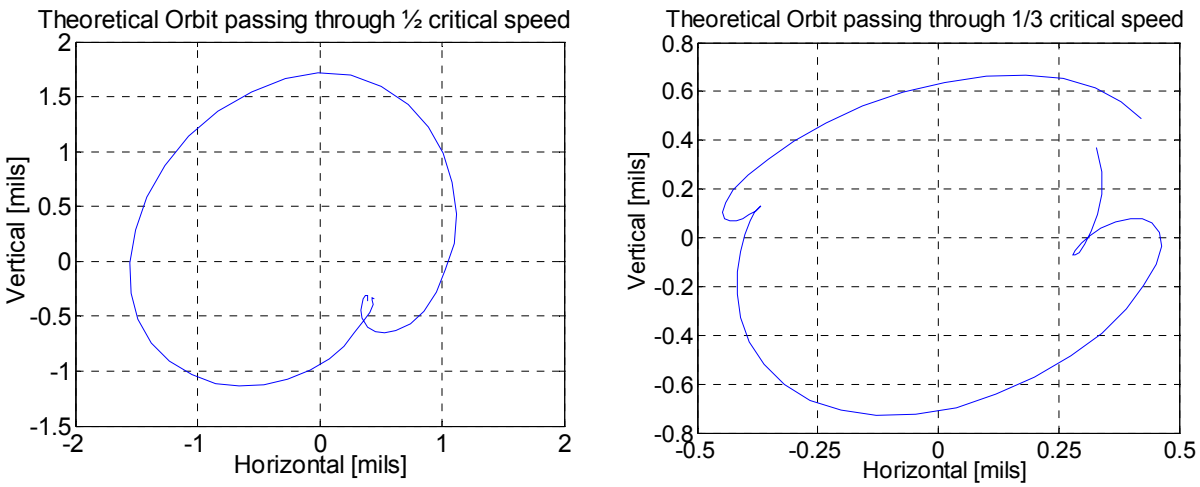

Figure 12 – Theoretical orbits for cracked rotor passing through ½ and 1/3 critical speed

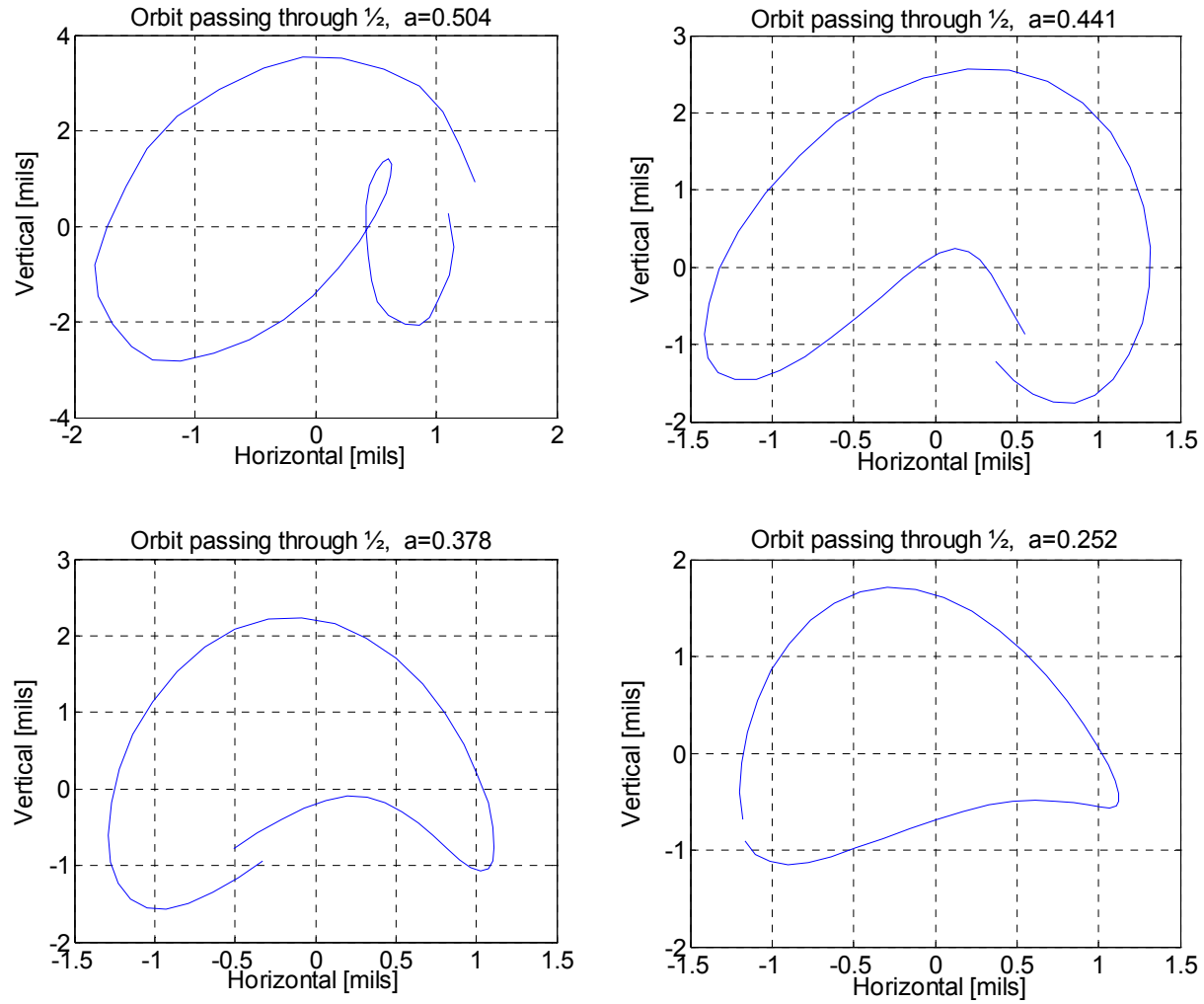

Figure 13 – Theoretical orbits for different crack severities

CONCLUSIONS

The sub-harmonic resonances were verified experimentally and it was found that passing through ½ critical speed corresponds to important changes in both the orbit and the time response in a cracked shaft as compared with the pristine condition. Changes in the natural frequencies were observed for the cracked shaft and the lowest stiffness occurs when the crack axis match with the axis used to evaluate the system response.

It must be considered however that the experimental crack used in the tests is not a real fatigue crack. Despite of that, the experimental results match satisfactorily the theoretical ones. This leads us to say that the Mayes' model is suitable for studying the dynamic behavior of cracked rotors. When the crack severity is less than 0.2, the changes in the rotor response are very slight, however further experimental work is to be performed to check if the model is still representative under these conditions. Also, further work will include a real fatigue crack in which it is expected that the breathing effect will have more influence in the rotor response.

The main contribution of this work is the derivation of the stiffness matrix and the algorithm to calculate the rotor response in transient motion. Other types of excitation forces (misalignment, for instance) should also be studied in cracked rotors. The influence of more than one crack along the shaft should also be in investigated.

REFERENCES

Anderson, T.L., 1995, "Fracture Mechanics Fundamentals and Applications", 2 ed. CRC Press.

Bathe, K.L.; Wilson, E.L., 1976, "Numerical Methods in Finite Element Analysis, Prentice-Hall".

Darpe, A.K.; Gupta, K., 2003, "Transient response and breathing behaviour of a cracked Jeffcot rotor", Journal of Sound and Vibration.

Dimarogonas, A.D.; Paipetis S.A., 1983, "Analytical Methods in Rotor Dynamics", London, Applied Science Publishers, 218p.

Gash, R., 1993, "A survey of the dynamic behavior of a simple rotor shaft with a transverse crack", Journal of sound and vibration. 62 (2), pp. 313-332.

Lalanne, M., Ferraris, G., 1998, "Rotordynamics Prediction in Engineering", 2. ed. N. Y, John Wiley and Sons.

Mayes, I.W., Davies, W.G.R., 1984, "The vibrational behavior of a multi-shaft, multi-bearing system in the presence of a propagating crack", ASME 146. Vol 106. Jan.

Nelson, H.D., Nataraj, C., 1986, "The Dynamics of a rotor system with a cracked shaft. Journal of Vibration, Acoustics, Stress and reliability in design", Vol 108. pp 189-196. Apr.

Oller, S., 2001, "Fractura Mecánica un enfoque global", Barcelona: CIMNE, 286p.

Pacheco, R.P., 1996, "Comportamento Transiente de Máquinas Rotativas", Dissertação de Mestrado – Universidade Federal de Uberlândia, MG

J.E.T.; Friswell, M.I., 2003, "The Dynamics of Rotating Machines with cracks. Materials Science Forum", Vol 440-441, pp 311-318.

Saavedra, P.N., Cuitiño, L.A., 2002, "Vibration Analysis of Rotor for crack identification. Journal of Vibration and Control". Vol 8, pp 51-67.

RESPONSIBILITY NOTICE

The author(s) is (are) the only responsible for the printed material included in this paper.